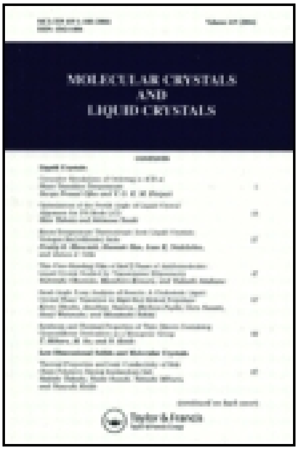

Molecular Crystals and Liquid Crystals
Publication details, including instructions for authors and subscription information:
http://www.tandfonline.com/loi/gmcl20

Crystalline-amorphous organic co-deposited films showing efficient photo-electric conversion

Kouji Suemori [a], Takahiro Miyata [a], Yuko Oishi [a], Masahiro Hiramoto [a] & Masaaki Yokoyama [a]
[a] Material and Life Science, Graduate School of Engineering, Osaka University, Yamadaoka, Suita, Osaka, Japan

Version of record first published: 18 Oct 2010

To cite this article: Kouji Suemori, Takahiro Miyata, Yuko Oishi, Masahiro Hiramoto & Masaaki Yokoyama (2004): Crystalline-amorphous organic co-deposited films showing efficient photo-electric conversion, Molecular Crystals and Liquid Crystals, 425:1, 181-188

To link to this article: http://dx.doi.org/10.1080/15421400490506757

Mol. Cryst. Liq. Cryst., Vol. 425, pp. 181/[459]–188/[466], 2004
Copyright © Taylor & Francis Inc.
ISSN: 1542-1406 print/1563-5287 online
DOI: 10.1080/15421400490506757

CRYSTALLINE-AMORPHOUS ORGANIC CO-DEPOSITED FILMS SHOWING EFFICIENT PHOTO-ELECTRIC CONVERSION

Kouji Suemori, Takahiro Miyata, Yuko Oishi, Masahiro Hiramoto, and Masaaki Yokoyama
Material and Life Science, Graduate School of Engineering, Osaka University, Yamadaoka, Suita, Osaka 565-0871, Japan

Magnitude of photocurrent density of the organic co-deposited films were revealed to be definitely affected by their nanostructure which can be controlled via the substrate temperature. Crystalline-amorphous nano-composites having individual transporting routes for electrons and holes showed the largest photocurrent irrespective of the combination of organic semiconductors.

Keywords: co-deposited films; crystalline-amorphous nano-composite; organic semiconductors; photo-electric conversion; substrate temperature

INTRODUCTION

Co-deposited films consisting of two kinds of organic semiconductors possess high potential for photocarrier generation. We have reported the p-i-n organic solar cells in which the i-interlayer is a co-deposited film of perylene and phthalocyanine pigments [1,2]. It is obvious, however, that the nanostructure of the co-deposited films crucially affects the photocurrent generation process. From this standpoint of view, we tried to control the structure of co-deposited films *via* controlling the substrate temperature during vacuum co-deposition.

In this paper, we report the relationship between the nanostructure of co-deposited films and their photovoltaic properties. Co-deposited films between phthalocyanines and perylene pigments (H_2Pc:Me-PTC,

Received 1 October 2003; accepted 23 March 2004

The authors are grateful to S. Ooki of Dainichi Seika Kogyo Inc. for kindly donating the perylene pigments.

Address correspondence to Kouji Suemori, Material and Life Science, Graduate School of Engineering, Osaka University, Yamadaoka, Suita, Osaka 565-0871, Japan. Tel.: +81-6-6879-7933, Fax: +81-6-6879-7934, E-mail: Suemori@chem.eng.osaka-u.ac.jp

CuPc:Im-PTC) [1–3] and between fullerene and H_2Pc (C_{60}:H_2Pc) [4–7] were examined. Photocurrent remarkably increased by forming the amorphous-crystalline nano-composites.

EXPERIMENTAL

Sandwich-type cells of co-deposited films (Fig. 1) were fabricated on indium tin oxide (ITO) glass substrates pre-treated by air plasma [8]. Co-deposited films were fabricated by the co-evaporation from two separately controlled sources. The mixing ratio of two semiconductors was kept at 1:1. Substrate temperature during the co-deposition was controlled by using a substrate heating-cooling unit (ULVAC, UHCS-1000).

Photovoltaic measurements were carried out under the irradiation of simulated solar light (92 mWcm^{-2}, Yamashita Denso, Co., Ltd., YSS-50A). Cross section of co-deposited films, which was exposed by cutting the glass substrate, was observed by using scanning electron microscope (SEM; Hitachi, S-4300SD). Crystallinity of co-deposited films was evaluated by X-ray diffractometer (XRD; Rigaku, RINT-2000).

RESULTS AND DISCUSSION

Figure 2 shows the current-voltage characteristics for C_{60}:H_2Pc co-deposited films. When the co-deposition was performed on the substrate

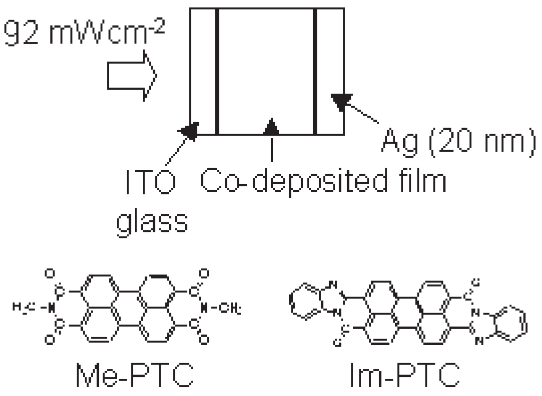

FIGURE 1 Sandwich-type cell of co-deposited films. Co-deposited films of Me-PTC:H_2Pc (thickness: 150 nm), Im-PTC:CuPc (400 nm), and C_{60}:H_2Pc (500 nm) were fabricated. Chemical formulas of perylene pigments are also shown. H_2Pc, CuPc, and C_{60} indicate metal-free phthalocyanine, copper phthalocyanine, and fullerene, respectively.

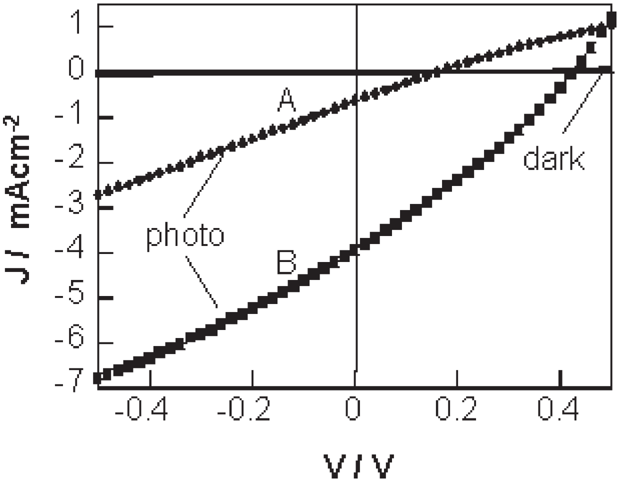

FIGURE 2 Current-voltage characteristics for C_{60}:H_2Pc (1:1) co-deposited films of the thickness of 500 nm. Co-deposition was performed on the substrate at +20°C (curve A) and at +80°C (curve B). Simulated solar light (92 mWcm^{-2}) was irradiated to the ITO electrode. Performance for curve B: $J_{sc} = 3.9$ mAcm^{-2}, $V_{oc} = 0.42$ V, FF = 0.29, Efficiency = 0.5%.

at room temperature, short-circuit photocurrent density (J_{sc}) was 0.6 mAcm^{-2} (curve A). Interestingly, when the co-deposition was performed on the substrate heated at +80°C, J_{sc} increased to 3.9 mAcm^{-2}. Photo-electric power conversion efficiency was 0.5%. Obviously, photovoltaic properties strongly dependent on the substrate temperature during co-deposition. Open-circuit photovoltage (V_{oc}) of 0.42 V of the direction of (+)ITO/C_{60}:H_2Pc/Ag(−) was observed. This value corresponds to the difference between the work function of ITO electrode (5.3 eV) and that of vacuum-deposited Ag film (4.9 eV) measured by Kelvin vibrating capacitor method [9].

Figure 3 summarizes the dependence of J_{sc} on the substrate temperature for Me-PTC:H_2Pc (curve A), Im-PTC:CuPc (curve B), and C_{60}:H_2Pc (curve C). Optimum temperature is dependent on the combination of organic semiconductors, namely, maximum J_{sc} was observed at −170, +50, and +80°C for Me-PTC:H_2Pc, Im-PTC:CuPc, and C_{60}:H_2Pc, respectively.

We determined the nanostructure of co-deposited films by using XRD and SEM. Here we describe the Im-PTC:CuPc case. Figure 4 shows XRD patterns for Im-PTC:CuPc films fabricated at various temperature. Individual Im-PTC and CuPc films fabricated at room temperature showed diffraction peaks at around 12° and 6°, respectively. Below +20°C, there were no

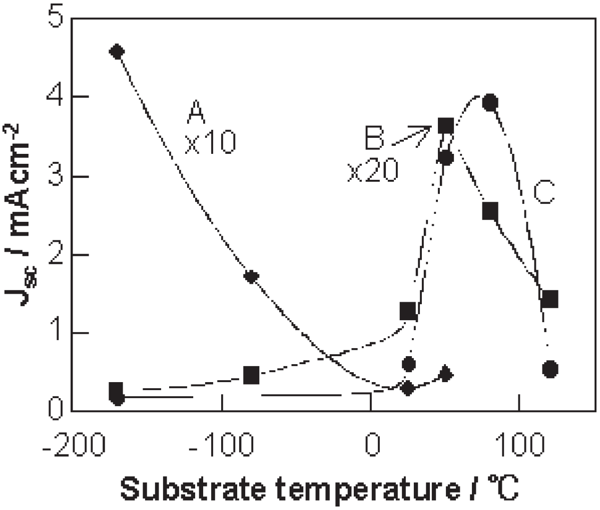

FIGURE 3 Dependence of J_{sc} on substrate temperature during co-deposition. Curves A, B, and C are for Me-PTC:H_2Pc, Im-PTC:CuPc, and C_{60}:H_2Pc, respectively. Ratio of pigments was 1:1. Simulated solar light (92 mWcm^{-2}) was irradiated to ITO electrode.

peaks. At +50°C, a broad CuPc peak was appeared while there was no Im-PTC peak. Above +80°C, both CuPc and Im-PTC peaks were observed. Namely, both CuPc and Im-PTC are amorphous in the temperature region from +20 to −170°C, CuPc is crystalline and Im-PTC is amorphous at around +50°C, and both CuPc and Im-PTC are crystalline in the temperature region from +80 to +120°C. Interestingly, the substrate temperature of +50°C which formed crystalline CuPc - amorphous Im-PTC co-deposited film coincides to that of photocurrent maximum (Fig. 3, curve B).

Figure 5 shows the SEM images of cross section of co-deposited films. At −170°C, entire cross section was smooth and there was no recognizable structure. At +50°C, a lot of grain was surrounded by smooth parts. At +120°C, smooth parts disappeared and only grains were observed. Based on XRD and SEM, we could depict the schematic illustrations of cross sectional structure sandwiched between ITO and Ag electrodes in Figure 6. At low temperature, Im-PTC and CuPc are mixed molecularly and forms an amorphous film [(a) molecular mixture]. At around +50°C, crystalline CuPc grains are surrounded by amorphous Im-PTC [(b) crystalline-amorphous nano-composite]. At high temperature, crystalline CuPc and crystalline Im-PTC are mixed [(c) crystalline-crystalline composite].

We also performed XRD and SEM measurements for Me-PTC:H_2Pc and C_{60}:H_2Pc. In the case of Me-PTC:H_2Pc, crystalline-amorphous

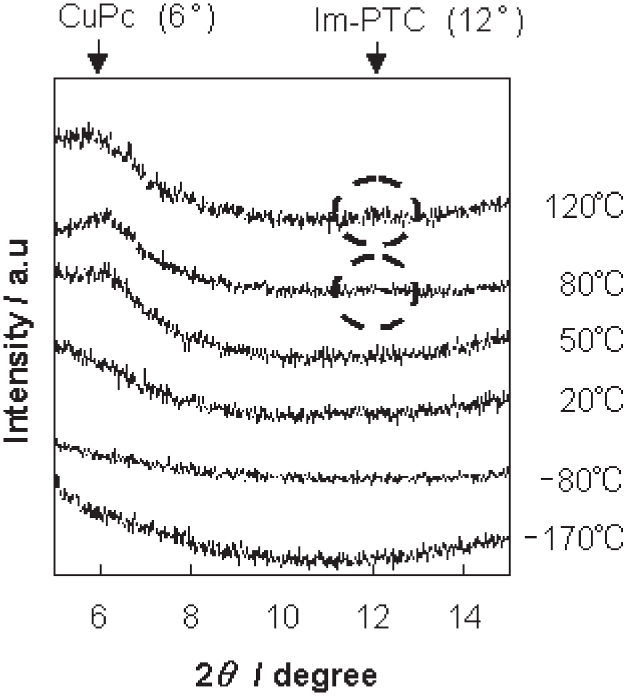

FIGURE 4 X-ray diffraction patterns for Im-PTC:CuPc (1:1) films co-deposited on the substrate at various temperature. Individual Im-PTC and CuPc films showed diffraction peaks at around 12° and 6°, respectively (arrows). Im-PTC peaks appeared at +80 and +120°C are inside the broken circles.

nano-composite and molecular mixture was confirmed to form at −170°C and at room temperature, respectively [10]. In the case of C_{60}:H_2Pc, crystalline-amorphous nano-composite was confirmed to form at around +80°C. Molecular mixture and crystalline-crystalline composite were confirmed to form at low temperature side and high temperature side, respectively. Although the optimum temperature is dependent on the semiconductor combination, crystalline-amorphous nano-composite is always formed at each optimum temperature. Therefore, we concluded that the formation of crystalline-amorphous nano-composite is essential to generate the largest photocurrent.

Since direct molecular contacts of Me-PTC/H_2Pc, Im-PTC/CuPc, and C_{60}/H_2Pc offer the photocarrier generation sites due to the exciton dissociation caused by the inter-molecular charge transfer, co-deposited films having vast number of molecular contacts possess a high potential for photocarrier generation. However, to generate photocurrent,

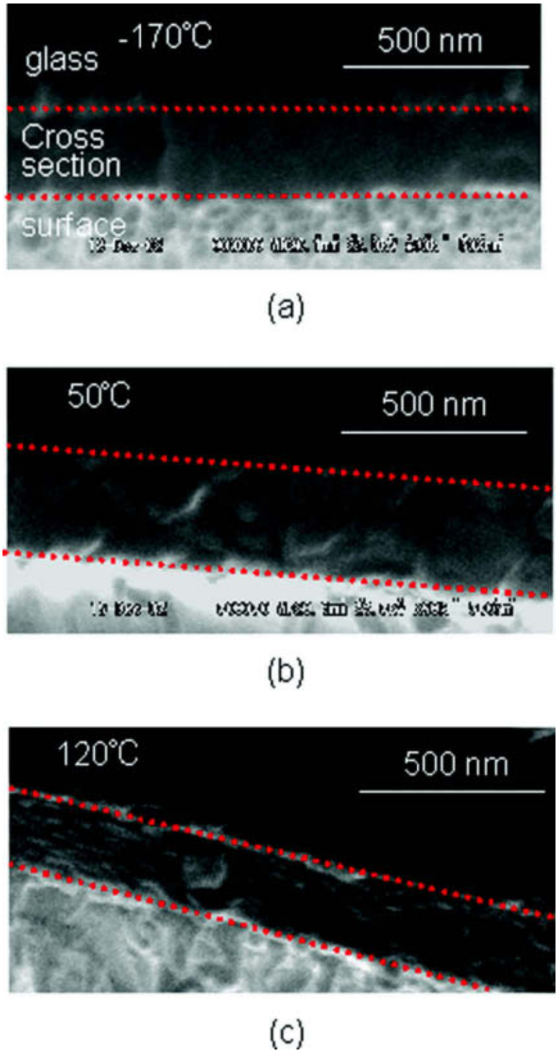

FIGURE 5 SEM images of the cross section of Im-PTC:CuPc (1:1) films fabricated on the substrates at −170°C (a), +50°C (b), and +120°C (c). Cross sections are in between broken lines.

photogenerated carriers should be transported to the electrodes. Efficient photocurrent generation in crystalline-amorphous nano-composite was concluded to be due to the formation of routes for electrons and holes, which allows spatially separated transport to respective electrodes (Fig. 6(b)). On the contrary, in the case of molecular mixture (Fig. 6(a)),

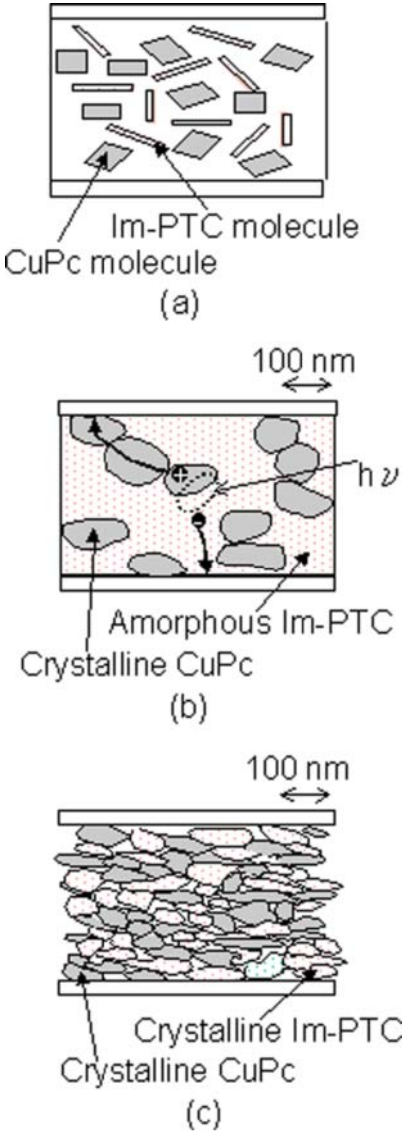

FIGURE 6 Schematic illustrations of cross sectional structures of co-deposited films. (a) Molecular mixture. (b) Crystalline-amorphous nano-composite. (c) Crystalline-crystalline composite. Figures 6(b) and (c) are illustrated by tracing the SEM images of Figures 5(b) and (c).

photogenerated electrons and holes easily encounter and recombine to disappear due to the absence of transport routes. In the case of crystalline-crystalline composite (Fig. 6(c)), increase of the number of distinct grain boundaries formed between nanocrystals seems to obstruct seriously the carrier transport.

REFERENCES

[1] Hiramoto, M., Fujiwara, H., & Yokoyama, M. (1991). *Appl. Phys. Lett.*, *58*, 1062.
[2] Hiramoto, M., Fujiwara, H., & Yokoyama, M. (1992). *J. Appl. Phys.*, *72*, 3781.
[3] Tang, C. W. (1986). *Appl. Phys. Lett.*, *48*, 183.
[4] Oishi, Y., Hiramoto, M., & Yokoyama, M. Extended Abstracts of the 48th Spring Meeting 2001. Japan Society of Applied Physics and Related Societies, 29a-ZG-7.
[5] Matsunobu, G., Oishi, Y., Yokoyama, M., & Hiramoto, M. (2002). *Appl. Phys. Lett.*, *81*, 1321.
[6] Peumans, P. & Forrest, S. R. (2001). *Appl. Phys. Lett.*, *79*, 126.
[7] Gebeyehu, D., Maennig, B., Drechsel, J., Leo, K., & Pfeiffer, M. (2003). *Solar Energy Materials and Solar Cells, 79,* 81.
[8] Furukawa, K., Terasaka, Y., Ueda, H., & Matsumura, M. (1997). *Synth. Metals*, *91*, 99.
[9] Hiramoto, M., Ihara, K., & Yokoyama, M. (1995). *Jpn. J. Appl. Phys.*, *34*, 3803.
[10] Hiramoto, M., Suemori, K., & Yokoyama, M. (2002). *Jpn. J. Appl. Phys.*, *41*, 2763.